Characterisation of two alcohol acyltransferases from kiwifruit (*Actinidia* spp.) reveals distinct substrate preferences

Catrin S. Günther [a,b], Christian Chervin [c], Ken B. Marsh [a], Richard D. Newcomb [a], Edwige J.F. Souleyre [a,*]

[a] *The New Zealand Institute for Plant & Food Research Ltd., Private Bag 92169, Auckland 1142, New Zealand*
[b] *Department of Chemistry, The University of Auckland, Private Bag 92019, Auckland, New Zealand*
[c] *UMR 990, Génomique et Biotechnologie des Fruits, INRA-INP/ENSAT, Université de Toulouse, BP 32607, 31326 Castanet, France*

A B S T R A C T

Volatile esters are key compounds of kiwifruit flavour and are formed by alcohol acyltransferases that belong to the BAHD acyltransferase superfamily. Quantitative RT-PCR was used to screen kiwifruit-derived expressed sequence tags with proposed acyltransferase function in order to select ripening-specific sequences and test their involvement in alcohol acylation. The screening criterion was for at least 10-fold increased transcript accumulation in ripe compared with unripe kiwifruit and in response to ethylene. Recombinant expression in yeast revealed alcohol acyltransferase activity for *Actinidia*-derived *AT1*, *AT16* and the phylogenetically distinct *AT9*, using various alcohol and acyl-CoA substrates. Functional characterisation of AT16 and AT9 demonstrated striking differences in their substrate preferences and apparent catalytic efficiencies (V'_{max} K_m^{-1}). Thus revealing benzoyl-CoA:alcohol *O*-acyltransferase activity for AT16 and acetyl-CoA:alcohol *O*-acyltransferase activity for AT9. Both kiwifruit-derived enzymes displayed higher reaction rates with butanol compared with ethanol, even though ethanol is the main alcohol in ripe fruit. Since ethyl acetate and ethyl benzoate are major esters in ripe kiwifruit, we suggest that fruit characteristic volatile profiles result from a combination of substrate availability and specificity of individual alcohol acyltransferases.

1. Introduction

Until thirty years ago plant secondary metabolites were mainly recognised as "metabolic waste products" (Peach, 1950). However this perspective has changed remarkably with more than 200,000 different compounds identified to date. These phytochemicals perform a variety of roles in plants from defence against abiotic and biotic stresses through to attraction and stimulation of its biological environment (Hartmann, 2007). A large number of these molecules are produced by acylation of a hydroxyl, amino or thiol-group, catalysed by acyltransferases (EC 2.3.1.x). Of particular importance are members of the BAHD (**b**enzyl alcohol-acetyl-, **a**nthocyanin-*O*-hydroxy-cinnamoyl-, anthranilate-N-**h**ydroxy-cinnamoyl/benzoyl-, **d**eacetyl-vindoline) acyltransferase (AT) superfamily that produce a wide range of functionally important compounds such as lignin, phenolics, alkaloids, phytoalexins, anthocyanins and volatile esters (St-Pierre and De Luca, 2000; D'Auria, 2006). BAHD ATs are generally recognised by their active site motif (HXXXD) and a conserved region (DFGWG) with likely structural significance (Ma et al., 2005). Like most ATs, BAHD proteins use Coenzyme A (CoA)-thioesters as acyl donors and one subgroup of BAHD ATs specifically forms esters by aliphatic or aromatic *O*-acylation of alcohol acceptor molecules.

Volatile esters produced by these alcohol acyltransferases (AATs) often drive plant-food recognition because they contribute to the "fruity" aroma of edible fruits. Some esters are also responsible for specific, key flavours or odours (Morton and Macleod, 1990). In kiwifruit, for example, elevated levels of methyl and ethyl butyrate have been recognised as characteristic fruit aroma compounds (Gilbert et al., 1996). Furthermore, these compounds dominate (Fig. 1) the fruit ester profiles of the commercial kiwifruit cultivars *Actinidia deliciosa* var. deliciosa 'Hayward' and *Actinidia* Planch. var. *chinensis* 'Hort16A' and reach peak levels at the soft end of their eating firmness range (Wang et al., 2011). Additional alkyl substituted esters, including (methylsulfanyl)alkanoate and benzoate esters, have been identified from the volatile profiles of 'Hayward' and 'Hort16A' kiwifruit (Young and Paterson, 1985; Friel et al., 2007; Günther et al., 2010; Wang et al., 2011). The major alcohol detected in fruit of these cultivars was ethanol (Fig. 1) with at least 50% of the resulting volatile esters being ethyl esters.

Although changes in kiwifruit ester profiles have been well researched in response to ethylene, harvest maturity and postharvest treatment (Young and Paterson, 1985; Günther et al., 2010, 2011; Wang et al., 2011), the genes involved in ester biosynthesis remain to be elucidated. As a result of an expressed sequence tag (EST)

* Corresponding author. Tel.: +64 99257110; fax: +64 99257001.
E-mail address: Edwige.Souleyre@plantandfood.co.nz (E.J.F. Souleyre).

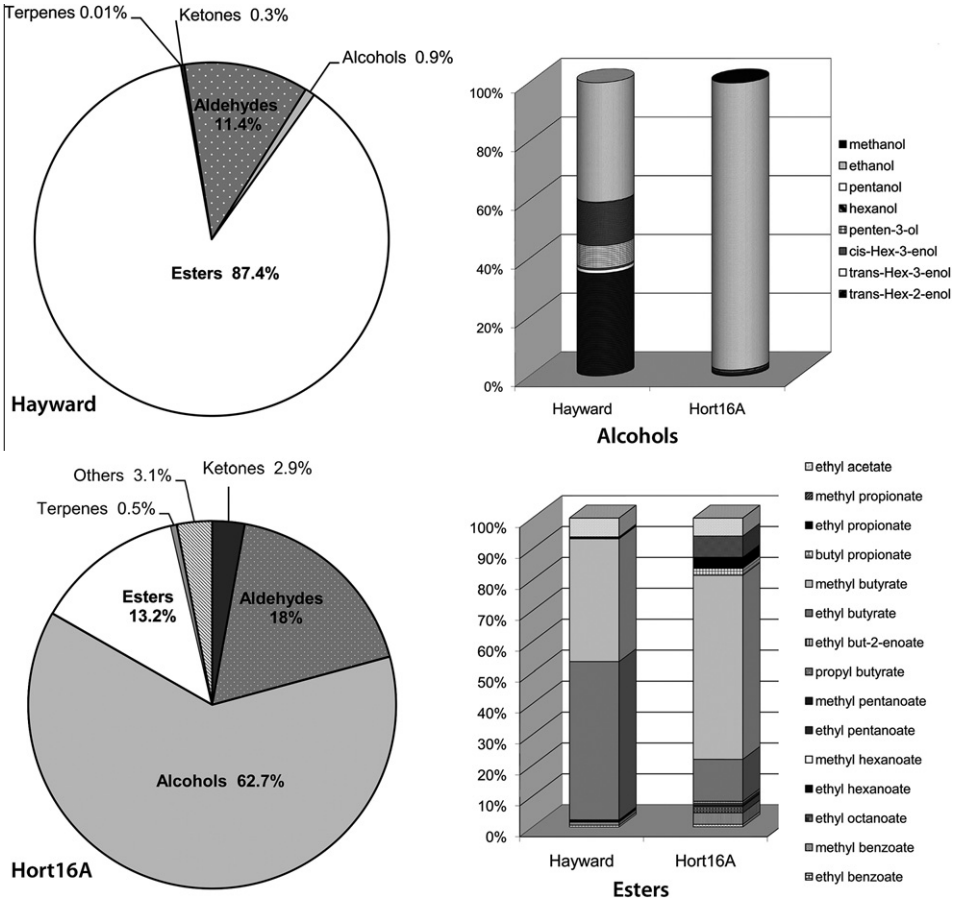

Fig. 1. Kiwifruit volatiles as% of total volatiles, alcohols as% of total alcohols, and esters as% of total esters. Volatile data for *Actinidia deliciosa* 'Hayward' were taken from "overripe" fruit (Young and Paterson, 1985). *Actinidia chinensis* 'Hort16A' volatile levels correspond to "soft" fruit as reported by (Friel et al., 2007). Alcohol and ester compounds are displayed in the same order as listed in keys to the right of the figure.

sequencing project from mainly four different *Actinidia* species (*A. deliciosa*, *A. chinensis*, *Actinidia arguta*, *Actinidia eriantha*) 25 full-length clones with putative AT and AAT functions have been identified (Crowhurst et al., 2008). Twelve of these contig-sequences were suggested to be flavour-related due to their phylogenetic relationship to characterised AATs from melon (CmAAT1, El-Sharkawy et al., 2005), apple (MpAAT1, Souleyre et al., 2005), banana (BanAAT, Beekwilder et al., 2004) and strawberry (SAAT and VAAT, Beekwilder et al., 2004).

Here, we investigated changes in steady-state transcript levels of *Actinidia* ATs to select sequences, potentially encoding for AATs that may be involved in ester biosynthesis, specific for ripe kiwifruit. We then studied the substrate preferences of these encoded enzymes using recombinant expression in order to evaluate their potential role for flavour-related fruit ester formation. Finally, the results are discussed in the light of their phylogenetic relationship with fruit and flower-derived AATs from other species.

2. Results and discussion

2.1. Isolation of putative ATs that are ripening-related using qRT-PCR analysis

Our previous studies (Günther et al., 2010, 2011) implied that enhanced volatile ester production during kiwifruit ripening was linked to ethylene-induced expression of *AATs*. Therefore, qRT-PCR analysis of *Actinidia* EST-contigs (Crowhurst et al., 2008) (all full-length-clones except for *AT15*) with putative AAT and AT-function was performed using RNA isolated from *A. deliciosa* 'Hayward' and *A. chinensis* 'Hort16A' that were softened to eating ripeness either with or without ethylene treatment as described in Nieuwenhuizen et al. (2007).

Ratios of the relative amounts of transcripts from ripe versus unripe fruit are displayed in Fig. 2. In *A. chinensis* 'Hort16A' (Fig. 2B) transcript levels of six contig sequences (*AT18*, *AT2*, *AT15*, *AT1*, *AT17*, *AT16*; isolated from *A. deliciosa*, *A. chinensis*, *A. arguta*) were 10 (*AT18*) to 550 (*AT15*) fold increased in ripe compared with unripe fruit, and 20 (*AT16*) to 2000 (*AT15*) fold after ethylene treatment. Except for *AT16*, transcript levels of these same contigs also differed from the majority of *ATs* in *A. deliciosa* 'Hayward' (Fig. 2A) showing 30 (*AT1*) to 100 (*AT18*) fold increased accumulation in ripe ethylene treated and untreated versus unripe fruit. Interestingly, transcript levels of *AT16*, which was isolated from *A. chinensis*, were only two-fold increased in ripe compared with unripe *A. deliciosa* 'Hayward' fruit and even two-fold decreased after ethylene-treatment. It has been suggested that *AT1*, *AT17* and *AT16* (Crowhurst et al., 2008) are orthologues, and it appears likely that ethylene regulation of *AT16* diverged upon speciation. Transcripts of *AT10* and *AT12*, isolated from *A. eriantha* and *A. deliciosa*, accumulated approximately five-fold in ripe 'Hort16A' but 15- and 40-fold in ethylene-treated 'Hayward' fruit, respectively. This suggests that the steady-state transcript levels of these sequences are likely to be ripening-related in *A. deliciosa*. Interestingly, transcript accumulation of *AT14*, *AT7*, *AT8* and *AT23* (isolated from *A. deliciosa* and *A. chinensis*) were lower or absent in 'Hayward' and 'Hort16A' fruit after ethylene treatment compared with unripe fruit. This suggests that this ripening hormone suppressed the expression of the corresponding genes, which

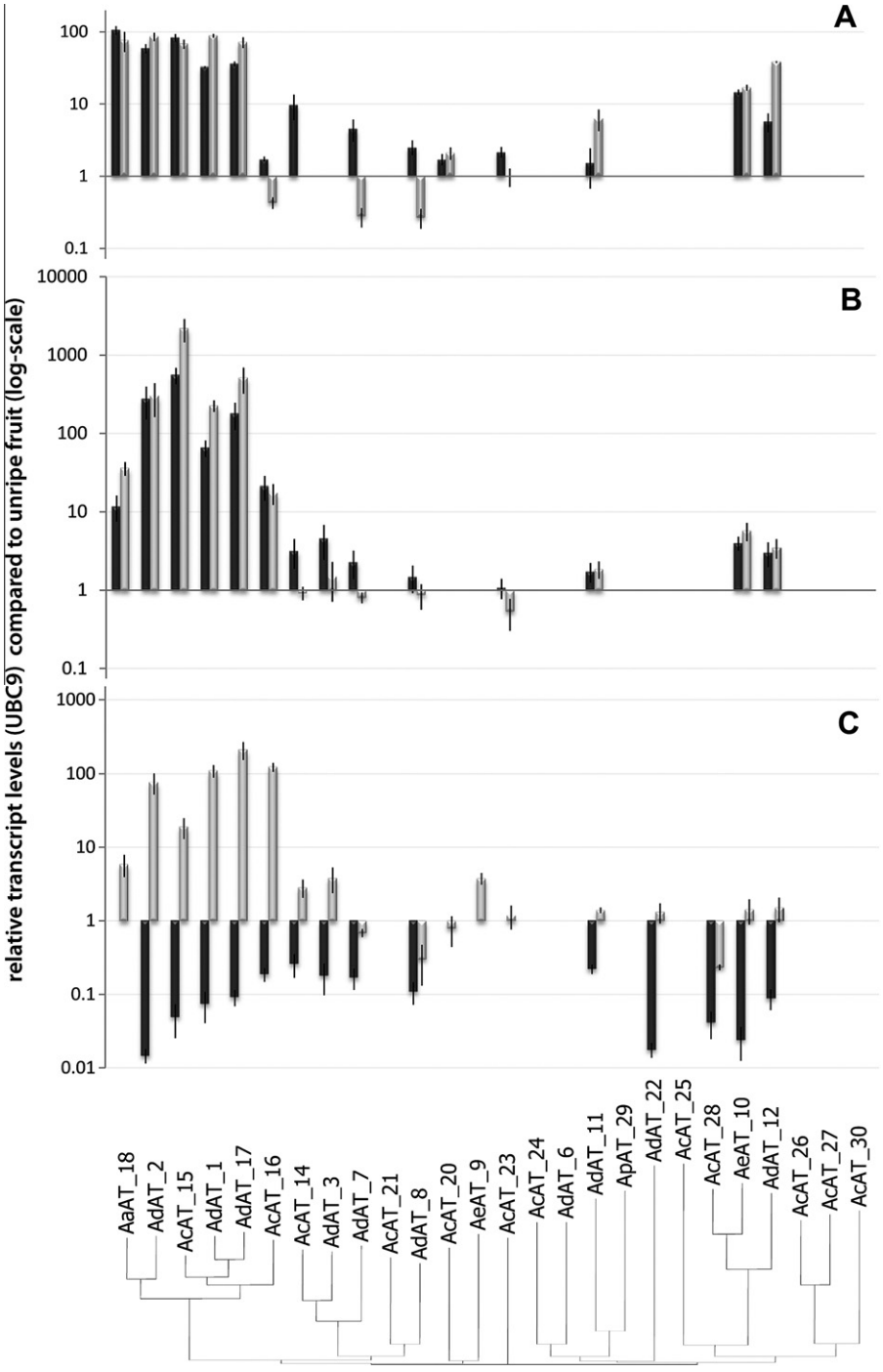

Fig. 2. Fold difference in transcript accumulation of *Actinidia*-derived contigs with proposed acyltransferase function in ripe compared with unripe fruit. (A) *Actinidia deliciosa* 'Hayward'; (B) *Actinidia chinensis* 'Hort16A'; (C) *Actinidia chinensis* ACO-RNAi (T1) fruit. Black bars display the transcript level ratio of ripe fruit without ethylene treatment to unripe fruit and grey bars display the ratio of ethylene-treated, ripe fruit to unripe fruit. The prefix indicates the species from which the sequence was originally isolated from (Aa: *A. arguta*, Ac: *A. chinensis*, Ad: *A. deliciosa*, Ae: *A. eriantha*, Ap: *A. polygama*). The error bars represent the standard deviation of the average of four technical replicates. Relative transcript levels are displayed on a $\log_{10}$ scale. Vector NTI® software was used to generate the phylogenetic tree (horizontal axis).

therefore do not appear to be involved in ethylene-stimulated fruit ester biosynthesis.

2.2. Identification of putative AATs from A. chinensis that are ethylene-induced

Because kiwifruit are regarded as climacteric fruit that exhibit a sharp peak in ethylene production (Whittaker et al., 1997), non-ethylene treated ripe fruit were likely to produce at least traces of this hormone. To provide evidence for the role of ethylene on *AT* and *AAT* expression in kiwifruit we monitored the steady-state transcript levels of their contigs in a 1-aminocyclopropane-1-carboxylic acid oxidase (ACO) silenced *A. chinensis* RNAi-line (T1) that did not produce detectable amounts of climacteric ethylene (Atkinson et al., 2011). This RNAi line was deficient in volatile ester production unless treated with exogenous ethylene (Atkinson et al., 2011).

It is demonstrated in Fig. 2C that little or no transcription of *AT18*, *AT2*, *AT15*, *AT1*, *AT17* and *AT16* was detectable from soft ACO-silenced kiwifruit but 130- (*AT16*) to 3400-fold (*AT17*) increased levels were observed after ethylene treatment, thus providing evidence that these particular genes are ethylene regulated. In ethylene-treated ACO-silenced T1 kiwifruit (Fig. 2C) transcript accumulations of five further sequences, (*AT14*, *AT3*, *AT22*, *AT10*, *AT12*) were 13- (*AT14*)–55-fold (*AT22*) higher compared with non-treated fruit but only up to three-fold increased in comparison to unripe fruit. Finally, transcript levels of *AT7* and *AT8* decreased during ripening and especially in response to ethylene as previously seen for 'Hayward' and 'Hort16A' kiwifruit (Fig. 2A and B). This suggests a potential role of these contigs for fruit development, which was supported by their accumulation in developing *A. chinensis* 'Hort16A' fruit and a further decline during fruit maturation (Supplemental data, Fig. S1). Hence, *AT18*, *AT2*, *AT15*, *AT1*, *AT17*, *AT16*, *AT10* and *AT12* were defined as ripening-related contigs due to increased transcript levels in ripe fruit and in response to ethylene as observed for ACO-RNAi T1, 'Hort16A' and 'Hayward' fruit. A flavour-related AAT-function was previously proposed for *AT18*, *AT2*, *AT15*, *AT1*, *AT17*, *AT16* (Crowhurst et al., 2008) but also for *AT9*, *AT23* and *AT22* which exhibited slightly increased transcript levels in ethylene-treated *A. chinensis* ACO-silenced (Fig. 2C) but not in 'Hort16A' or 'Hayward' fruit.

2.3. AAT-activity was confirmed for Actinidia ESTs using recombinant expression

The recombinant expression of proposed kiwifruit *AAT*s in yeast yielded soluble proteins at their predicted weights (AT1, 51 kDa; AT16, 51.98 kDa; AT9, 47.67 kDa; Supplemental data, Fig. S2A–C) that were similar to the predicted or actual sizes of most plant-derived ATs from the BAHD superfamily (St-Pierre and De Luca, 2000). The recombinant enzymes were then tested for AAT-function by measuring their ability to produce esters from a mixture containing alcohol and acyl-CoA substrates (Fig. 3). This experimental set-up was chosen to imitate a potential *in vivo* situation in which different substrates are available at the same time. From this mixture the major ester formed by AT1 (Fig. 3A) and AT16 (Fig. 3B) was butyl benzoate (53–55%), and by AT9 (Fig. 3C) was butyl acetate (45.6%). The general profile of esters produced by recombinant AT1 and AT16 was similar. This is perhaps not too surprising given that *AT1* which was isolated from *A. deliciosa* and *AT16* from *A. chinensis* are likely orthologues (Crowhurst et al., 2008). However, butyl butyrate production by AT1 was 4-times higher compared with AT16, whereas butyl 3-(methylsulfanyl)propionate formation was five-fold lower (Fig. 3A and B). Acetyl-CoA and propionyl-CoA were barely used as substrates for volatile ester production (less than 1.5%) by AT1 and AT16, but AT9 in contrast, predominantly formed acetate and propionate esters (Fig. 3C). Benzoate esters were not detected from recombinant AT9 and its ester profile comprised only 0.1% butyl 2-(methylsulfanyl)acetate. Due to their striking differences in ester production AT16 and AT9 were chosen for further functional studies.

2.4. Functional characterisation revealed benzoyltransferase activity for AT16 and acetyltransferase activity for AT9

The catalytic properties of recombinant AT16 and AT9 were evaluated in two ways. First by a screen for preferred substrates, using either individual alcohols with a mixture of eight different CoA-thioesters (Fig. 4A and C) or individual acyl-CoAs with a mixture of four alcohols (Fig. 4B and D). These substrate combinations were chosen according to esters previously found in kiwifruit (Young and Paterson, 1985; Friel et al., 2007; Günther et al., 2010; Wang et al., 2011). As presented in Fig. 4A, AT16 utilised C_1–C_4 straight chain alcohols. However, individual alcohols appeared to influence the acylation reaction carried out by the enzyme: all acyl-CoA substrates, tested in this study, were utilised for ester formation with butanol, whereas methyl esters were only formed with benzoyl- and 2-(methylsulfanyl)acetyl-CoA. Generally, the number and amount of volatile esters, produced by AT16, increased with increasing carbon-chain length of the alcohol acceptor molecule (Fig. 4A). From a mix of alcohols AT16 primarily catalysed butyl ester formation (Fig. 4B), with the highest enzyme activities observed for butanol with benzoyl-CoA and (methylsulfanyl)alkyl-CoAs. Thus, indicating a preference for these latter substrates for AT16. In comparison, AT9 produced butyl acetate and butyl propionate with highest catalytic activities (Fig. 4D), suggesting the preferred conversion of butanol with acetyl-CoA and propionyl-CoA. In contrast to AT16, benzoyl-CoA was utilised only in the absence of alternative acyl-CoA substrates by AT9 (Fig. 4D) and 3-(methylsulfanyl)propionate ester formation was not detected at all (Fig. 4C and D). In general, AT9 appeared to be more selective towards alcohols with an even-number of carbon atoms (Fig. 4C), except for propanol with acetyl-CoA. Ethyl esters were primarily formed with hexanoyl- and octanoyl-CoA.

Next, the apparent catalytic efficiency (ACE), defined as the initial velocity of the substrate response curve ($V'_{max}\,K_m^{-1}$ where V'_{max} is the apparent V_{max} of the semi-purified extract) was calculated for those substrates leading to highest ester production rates. It becomes clear for AT16 (Table 1) that the ACE for benzoyl-CoA was five-fold higher using butanol compared with ethanol. Furthermore, if butanol was present as a co-substrate, benzoyl-CoA was utilised at 15- and 20-fold higher reaction rates than butyl 3-(methylsulfanyl)propionate and butyl 2-(methylsulfanyl)acetate, respectively. We therefore conclude that the ACE of AT16 is highest for benzoyl-CoA and butanol under the conditions applied in this study. Even though benzoate ester levels in ripe 'Hayward' and 'Hort16A' kiwifruit are low compared with methyl and ethyl butyrate, they form a major part of the volatile ester profiles of these commercial cultivars (Fig. 1). AT16 is likely to play a role in the production of benzoate esters and also to contribute to (methylsulfanyl)alkanoate ester biosynthesis in ripe *A. chinensis* fruit. The finding that AT16 preferentially produced butyl esters *in vitro* does not diminish its role in the *in vivo* synthesis of ethyl esters, which dominate the kiwifruit volatile profiles (Young and Paterson, 1985; Friel et al., 2007; Günther et al., 2010). This may be explained by substrate availability of ethanol, the dominating alcohol present in 'Hort16A' kiwifruit (97%, Fig. 1). Substrate availability *in vivo* may also explain the elevated amounts of butyrate esters, but there is limited information about physiological butanoyl-CoA-levels in kiwifruit and it is also possible that other contigs, perhaps *AT2* or *AT15*, which have their highest transcript levels in ripe kiwifruit, encode proteins with high specificity for this substrate.

AT9, in comparison, also preferred butanol over ethanol with a 70-fold higher ACE for butyl acetate compared with ethyl acetate (Table 1). The $V'_{max}\,K_m^{-1}$ value for the formation of the enzyme's second major ester, butyl propionate, was two-fold lower compared with butyl acetate. Butyl acetate was reported as the major fruit ester identified in *A. eriantha* genotypes (Crowhurst et al., 2008), providing evidence for a role for AT9 in ester formation for this species, from which it was isolated. However, considerable amounts of acetate and propionate esters are also produced in the commercial kiwifruit cultivars (Fig. 1) and an orthologue of AT9 has recently been discovered in *A. chinensis* and *A. deliciosa* kiwifruit by us, suggesting the involvement of this enzyme in the generation of volatile esters in ripe fruit of these commercial cultivars. In comparison with AT16, the ACE of AT9 for 2-(methylsulfa-

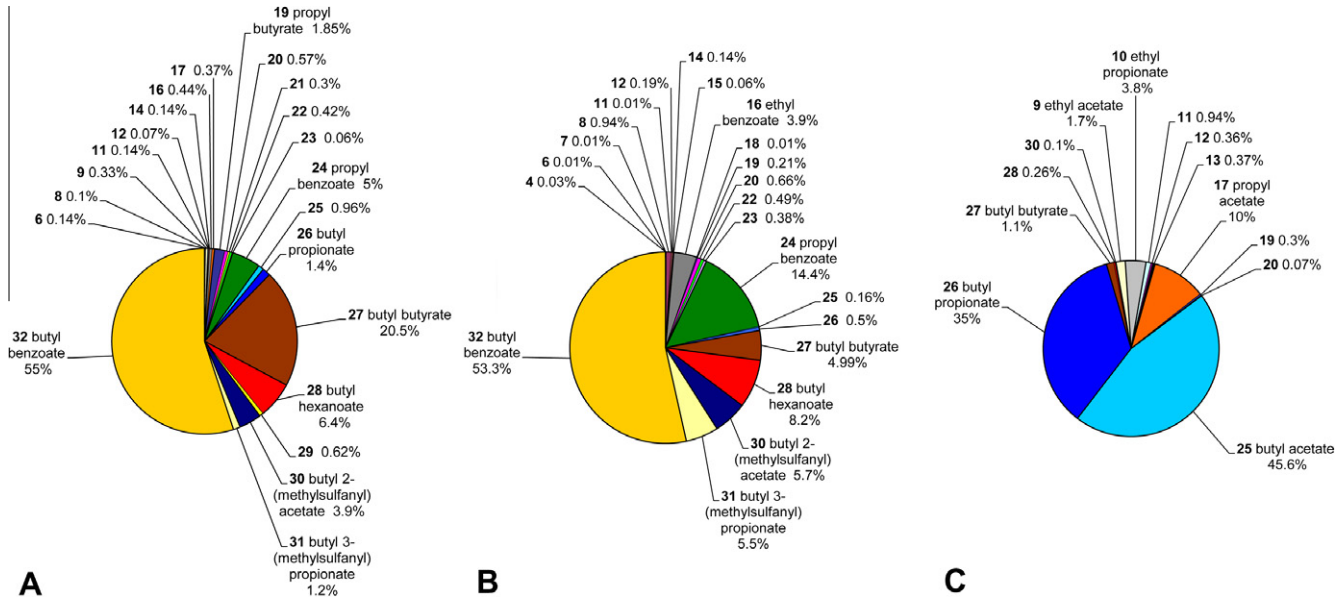

Fig. 3. Volatile esters produced by recombinant alcohol acyltransferases expressed in *Saccharomyces cerevisiae*. Levels of individual esters are displayed as the average% of total esters produced from a mixture of alcohol and acyl-CoA substrates ($n = 2$). A AT1; B AT16; C AT9. **1** Methyl acetate; **2** Methyl propionate; **3** Methyl butyrate; **4** methyl hexanoate; **5** methyl octanoate; **6** methyl 2-(methylsulfanyl)acetate; **7** methyl 3-(methylsulfanyl)propionate; **8** methyl benzoate; **9** ethyl acetate; **10** ethyl propionate; **11** ethyl butyrate; **12** ethyl hexanoate; **13** ethyl octanoate; **14** ethyl 2-(methylsulfanyl)acetate; **15** ethyl 3-(methylsulfanyl)propionate; **16** ethyl benzoate; **17** propyl acetate; **18** propyl propionate; **19** propyl butyrate; **20** propyl hexanoate; **21** propyl octanoate; **22** propyl 2-(methylsulfanyl)acetate; **23** propyl 3-(methylsulfanyl)propionate; **24** propyl benzoate; **25** butyl acetate; **26** butyl propionate. **27** butyl butyrate; **28** butyl hexanoate; **29** butyl octanoate; **30** butyl 2-(methylsulfanyl)acetate; **31** butyl 3-(methylsulfanyl)propionate; **32** butyl benzoate.

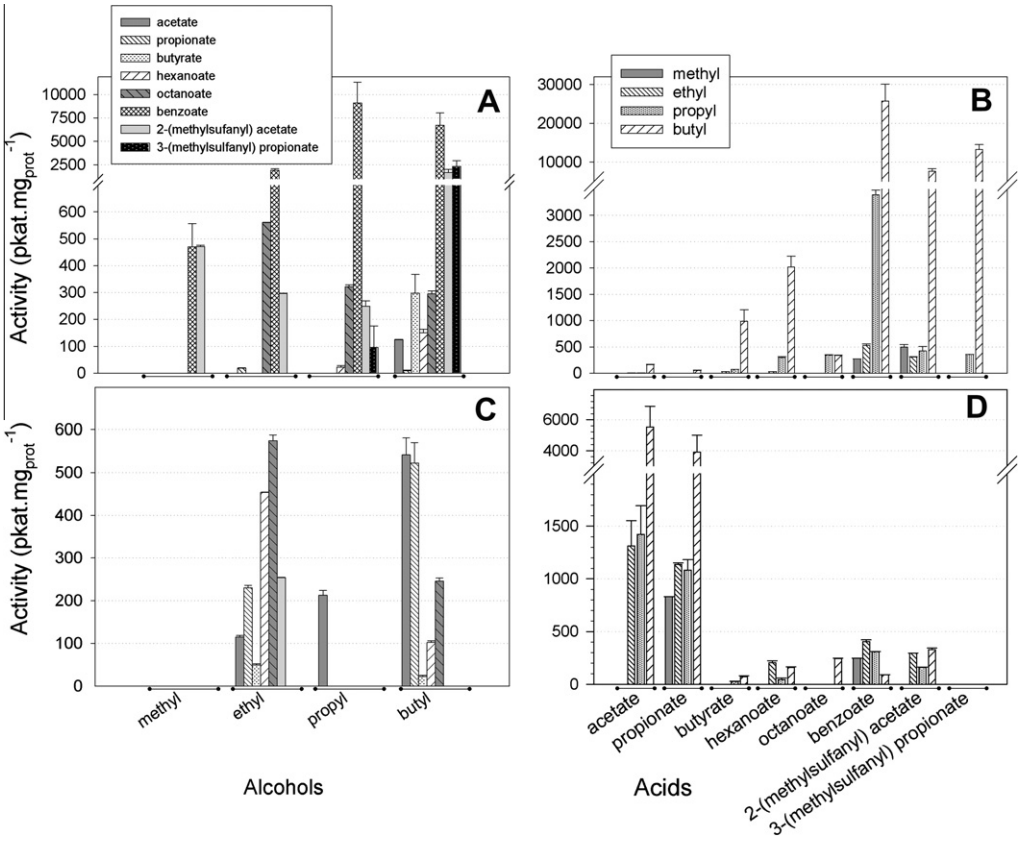

Fig. 4. Specific activity of recombinant alcohol acyltransferases (AAT) from kiwifruit. Panels A and B display the ester production rate of AT16, while panels C and D show AAT-activity of AT9. Recombinant protein was incubated with individual alcohol substrates and a mix of acyl-CoAs (A and C) or with individual acyl-CoAs and a mix of different alcohols (B and D), respectively. The error bars represent the standard deviation of the average of two replicates.

Table 1
Apparent catalytic efficiencies of recombinant *Actinidia* alcohol acyltransferases with preferred substrates.

	V'_{max} K_m^{-1} (nkat mg^{-1} μM^{-1})	
	AT16	AT9
Acetyl-CoA + ethanol	NA	1.2 ± 0.4
Acetyl-CoA + butanol	BQT	71.1 ± 1.2
Propionyl-CoA + butanol	NA	33.5 ± 1.1
2-(methylsulfanyl)Acetyl-CoA + butanol	8.2 ± 0.4	1.3 ± 0.1
3-(methylsulfanyl)propionyl-CoA + butanol	12.9 ± 3.1	NA
Benzoyl-CoA + ethanol	27.5 ± 2.0	NA
Benzoyl-CoA + butanol	157.7 ± 6.5	BQT

NA: not analysed; BQT: below quantification threshold.

nyl)acetyl-CoA with butanol (Table 1) was eight-fold lower, suggesting that this enzyme is not important for the generation of (methylsulfanyl)alkanoate esters.

2.5. Phylogenetic analysis and sequence alignment studies uncovered potential regions involved in acetyl- versus benzoyl-CoA preference

The kiwifruit AATs described here are members of the BAHD superfamily. They share the common features of plant ATs (D'Auria, 2006), including an active site motif HXXXD (amino acids 186–190, Fig. 5) and the conserved motif DFGWG (amino acids 455–460, Fig. 5) with likely structural function. Two major clades of functionally characterised BAHD AATs were defined using alignment (Fig. 5) and phylogenetic (Fig. 6) studies of *Actinidia* AATs with flavour- and scent-related AATs from other plant species. Most members from clade 1 prefer benzoyl-CoA and may consequently be classified as benzoyl-CoA:alcohol *O*-benzoyltransferases while those from clade 2 were previously characterised as acetyl-CoA:alcohol *O*-acyltransferases (D'Auria, 2006). However, functional data are somewhat incomplete. For example, the catalytic activity for benzoyl-CoA remains to be tested for MpAAT1 and all CmAATs (clade 1 and 2). Phylogenetically, AT9 from *Actinidia* and BanAAT appeared to be less closely related to the majority of clade 1 AATs (Fig. 6) which is also reflected in their substrate preference for acetyl-CoA. This dissociation is apparent from a lower degree of conservation found in the key motifs of clade 1 AATs and also in the novel motifs described below:

The benzoyl-CoA preferring AT16 and its relatives (AT1, AT17 Souleyre et al., 2011) display a HTMSD active site motif (Fig. 5, amino acids 186–190) that can be extended to $FAX_1RLNHTMX_2D$ (amino acids 180–190; with X_1 = Leu or Ile and X_2 = Ser or Ala) for benzoyl-CoA *O*-acyltransferases from kiwifruit and other species like papaya (VpAAT1, Balbontín et al., 2010), *Clarkia breweri* (CbBEBT, D'Auria et al., 2002), *Petunia* (BPBT, Boatright et al., 2004), apple (MpAAT1, Souleyre et al., 2005) and melon (CmAAT3, El-Sharkawy et al., 2005). This key motif is different compared with the acetyl-CoA preferring *Actinidia* AAT (AT9) in that His^{186} and Asp^{190} are the only conserved amino acids in this region. The novel motif PLLLIQVT (amino acids 164–171) was identified in close proximity to the active site motif for members of clade 1 (Fig. 5) but not for AT9, BanAAT and clade 2 proteins. In addition, AT9 also contains a single amino acid substitution in the highly conserved DFGWG motif (aromatic Trp^{459} is replaced by aliphatic Leu). Furthermore, the conserved Thr^{309} that has been shown to impact catalytic AAT activity in *Cucumis melo* (El-Sharkawy et al., 2005) is replaced by a Ser in AT9 but not in AT16, AT1 and AT17 from kiwifruit. The motif YYPLAGRL (amino acids 95–102) at the N terminus of the protein was recently described (Balbontín et al., 2010) and appears to be embedded in a region consisting of 39 amino acids (amino acids 91–130) that are mainly conserved for clade 1 AATs. However, whether these conserved motifs determine substrate specificity of the enzyme would need to be investigated using site-directed mutagenesis experiments combined with functional studies using key substrate combinations.

3. Conclusions

The transcript accumulation of six *Actinidia*-derived EST-sequences (*AT18*, *AT2*, *AT15*, *AT1*, *AT16*, *AT17*) was ethylene-regulated and specific for ripe 'Hort16A' and 'Hayward' (except AT16) kiwifruit, as demonstrated by qRT-PCR analysis. We provide evidence that recombinant AT1, AT16 and AT9 exhibit AAT-activity with a broad range of alcohol and acyl-CoA substrates leading to the formation of volatile esters commonly found in kiwifruit. In particular, AT16 and AT9 showed a preference for butanol as an alcohol acceptor molecule in combination with most acyl-CoAs, but AT16 was more specific towards benzoyl-CoA and (methylsulfanyl)alkyl-CoAs. In contrast, AT9 displayed a clear preference towards short-chain aliphatic-CoAs, namely acetyl-CoA and propionyl-CoA. On closer evaluation of protein sequence differences we identified conserved motifs in benzoyl-CoA:alcohol *O*-benzoyltransferases which may be involved in the CoA-substrate preference and may be useful for the classification of flavour-related AATs in the future.

4. Experimental

4.1. General experimental procedures

An autosampler with cooling rack (Gerstel MPS, Germany) was utilised for automated HS-SPME. PDMS-DVB fibre (65 μm, 23-gauge, Supelco, Bellefonte, USA) equilibration and sampling times of 5 min at 40 °C were deemed suitable. Volatiles were then thermally desorbed from the HS-SPME fibre in the injection port at 240 °C with a 2:1 split during transfer onto a 30 m × 0.25 mm × 0.25 μm film thickness DB-Wax (J & W Scientific, Folsom, CA, USA) capillary column in a HP6890 GC (Agilent Technologies, Santa Clara, CA, USA). The GC oven temperature program was 40 °C for 2 min, to 200 °C at 5 °C min^{-1}, and hold 2 min. The He-carrier gas flow was 1.5 ml min^{-1}, and the transfer line temperature was kept at 280 °C. The GC was coupled to a TOF-MS (Leco Pegasus III, St. Joseph, MI, USA) with an ion source temperature of 230 °C and 70 eV for electron impact ionisation. Ion spectra from 26 to 350 amu were collected with a data acquisition rate of 20 Hz. The total ion chromatograms were processed using the LECO chromaTOF software.

Authentic reference compounds were used for ester identification and quantification using a standard dilution series (1–10 μM $R^2 \geqslant 0.985$) in 0.1 M sodium phosphate buffer (pH 8) with 1% SDS (w/v). The repeatability of eight samples containing equal amounts of reference compounds was within 10% relative standard deviation if peak areas of esters with C_2–C_4 acyl-moiety were corrected against [D5]ethyl butyrate and the remaining ones against ethyl 3-([D3]-methylsulfanyl)propionate as internal standards. Because reference compounds were unavailable for propyl hexanoate, propyl octanoate and propyl benzoate, those compounds were quantified in equivalents of their corresponding ethyl esters.

Unless stated otherwise all chemicals, including alcohols (methanol, ethanol, propanol, butanol) authentic standards (methyl acetate, methyl propionate, methyl butyrate, methyl hexanoate, methyl octanoate, methyl benzoate, methyl 2-(methylsulfanyl)acetate, methyl 3-(methylsulfanyl)propionate, ethyl acetate, ethyl propionate, ethyl butyrate, ethyl hexanoate, ethyl octanoate, ethyl benzoate, ethyl 2-(methylsulfanyl)acetate, ethyl 3-(methylsulfanyl)propionate, propyl acetate, propyl propionate, propyl butyrate, propyl hexanoate, propyl benzoate, butyl

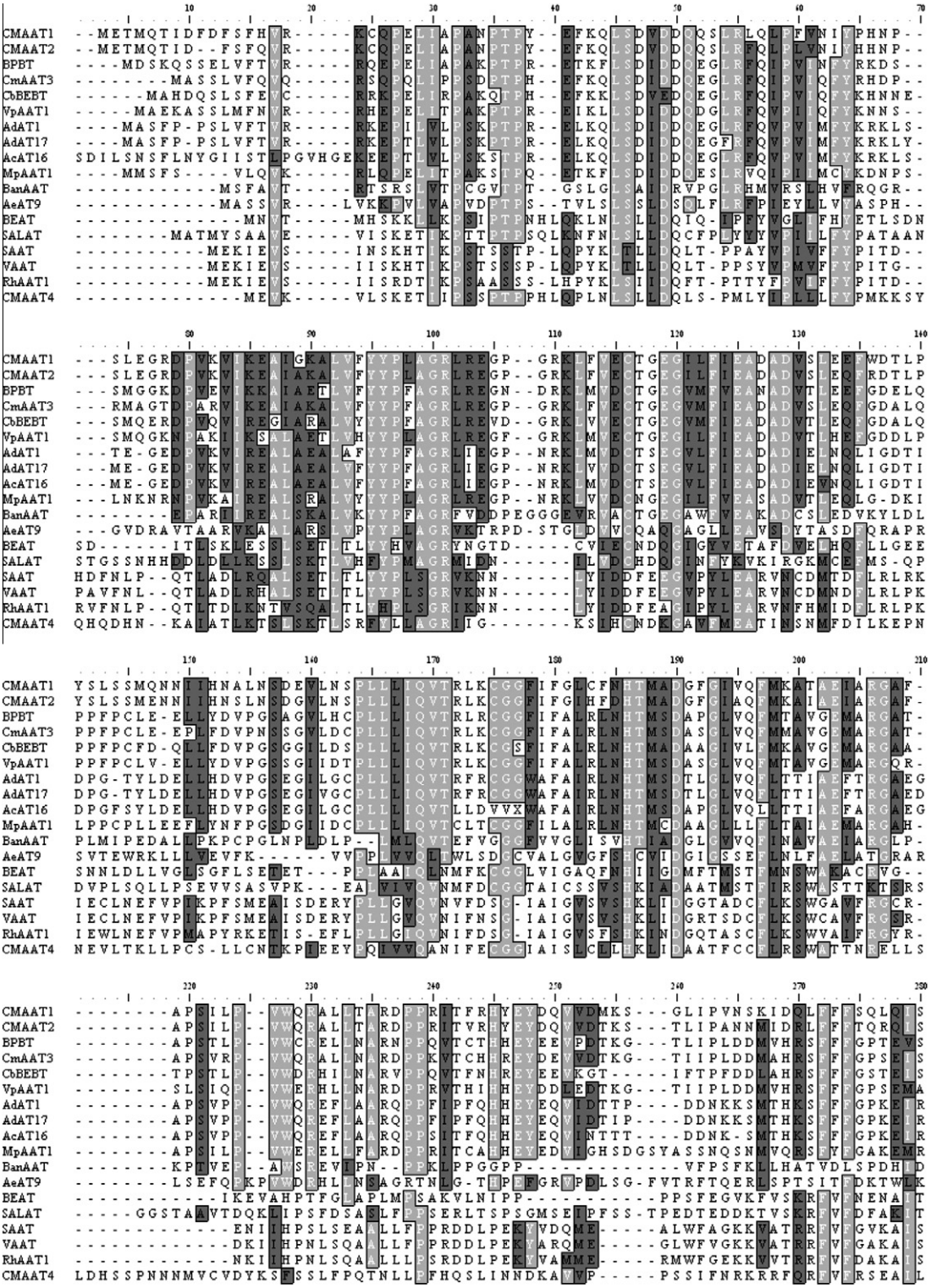

Fig. 5. Amino acid sequence alignment of four *Actinidia* alcohol acyltransferases (AATs) with fruit- or flower-derived AATs from different plant species. Abbreviations for species, acyltransferase (AT) names, and their GenBank accessions are as follows: AdAT1 (*Actinidia deliciosa* AT; HO772635); AdAT17 (*A. deliciosa* AT; HO772638); AcAT16 (*A. chinensis* AT; HO772640); AeAT9 (*A. eriantha* AT; HO772637); BEAT (*Clarkia breweri* acetyl-CoA:benzylalcohol acetyltransferase; AF043464 (Dudareva et al., 1998)); CbBEBT (*C. breweri* benzoyl-CoA:benzyl alcohol benzoyl transferase; AF500200 (D'Auria et al., 2002)); BPBT (*Petunia x hybrida* benzoyl-CoA:benzyl alcohol/phenylethanol benzoyltransferase; AAU06226 (Boatright et al., 2004)); MpAAT1 (*Malus pumila* alcohol acyltransferase; AY707098 (Souleyre et al., 2005)); CMAAT1 (*Cucumis melo* alcohol acyltransferase; CAA94432 (El-Sharkawy et al., 2005)); CMAAT2 (*C. melo* alcohol acyltransferase; AAL77060 (El-Sharkawy et al., 2005)); CMAAT3 (*C. melo* alcohol acyltransferase; AAW51125 (El-Sharkawy et al., 2005)); CMAAT4 (*C. melo* alcohol acyltransferase; AAW51126 (El-Sharkawy et al., 2005)); SAAT (*Fragaria* × *ananassa* alcohol acyltransferase; AAG13130 (Aharoni et al., 2000)); VAAT (*Fragaria vesca* alcohol acyltransferase; AX025504 (Beekwilder et al., 2004)); BanAAT (*Musa acuminata* alcohol acyltransferase; AX025506 (Beekwilder et al., 2004)); SALAT (*Papaver somniferum* salutaridinol 7-*O*-acetyltransferase; AF339913 (Grothe et al., 2001)); VpAAT1 (*Vasconcellea pubescens* alcohol acyltransferase; FJ548611 (Balbontín et al., 2010)); RhAAT1 (*Rosa hybrid* acetyl CoA geraniol/citronellol acetyltransferase; AAW31948 (Shalit et al., 2003)).

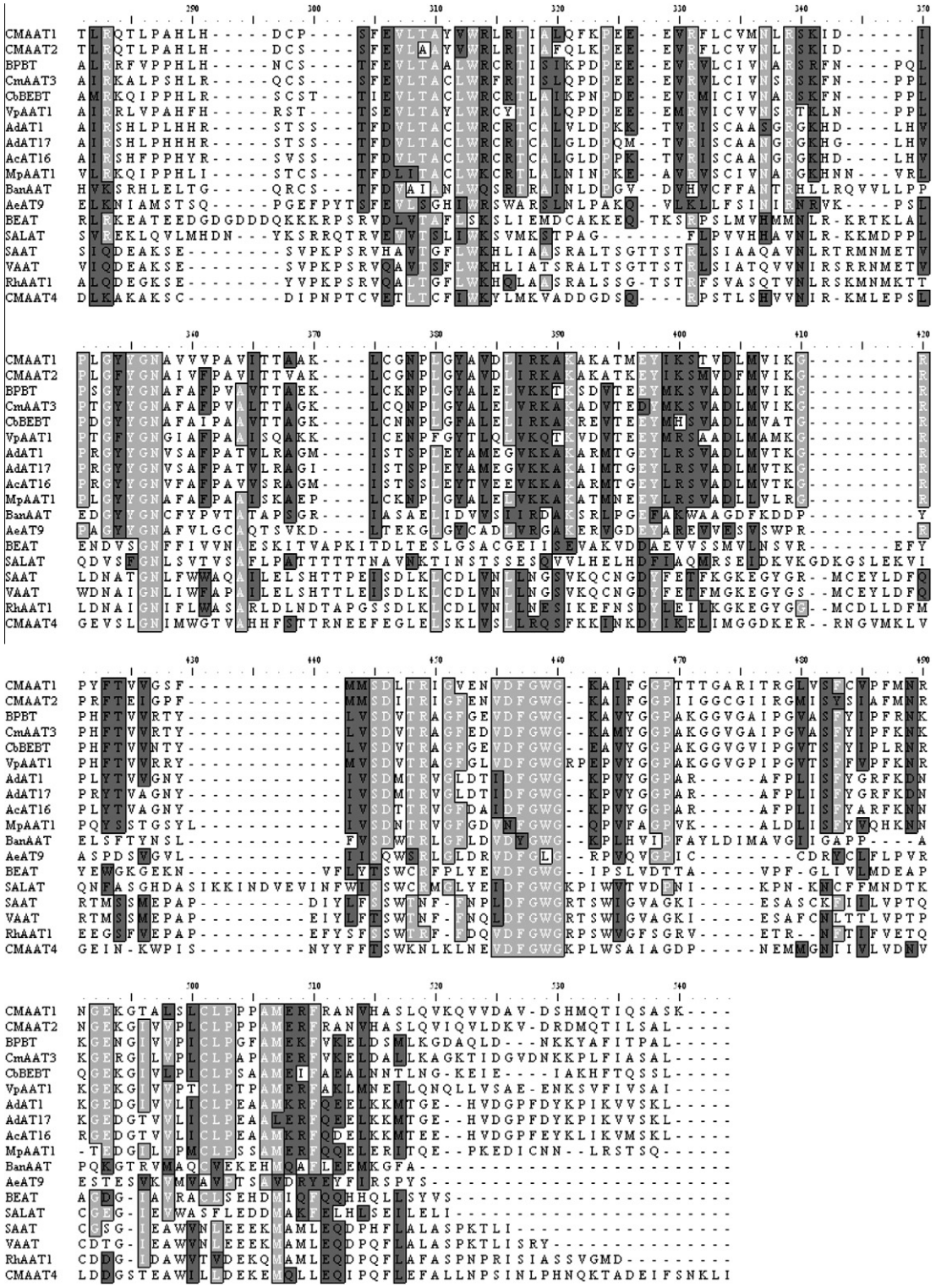

Fig. 5 (*continued*)

acetate, butyl propionate, butyl butyrate, butyl hexanoate, butyl octanoate, butyl benzoate) and CoA-thioesters (acetyl-CoA, propionyl-CoA, butyryl-CoA, hexanoyl-CoA, octanoyl-CoA, benzoyl-CoA) were purchased from Sigma-Aldrich New Zealand Ltd.

The reference compounds propyl and butyl 3-(methylsulfanyl)propionate and 2-(methylsulfanyl)acetate, the internal standards ethyl 3-([D3]methylsulfanyl)propionate and [D5]ethyl butyrate and the substrates 2-(methylsulfanyl)acetyl-CoA and 3-(methylsulfanyl)propionyl-CoA were synthesised as described previously (Günther et al., 2010, 2011).

4.2. Quantitative real-time RT-PCR (qRT-PCR) analysis

Levels of steady-state transcripts for 26 *Actinidia* AT ESTs (Crowhurst et al., 2008) were determined using cDNA made either from *A. chinensis* 'Hort16A' or *A. deliciosa* 'Hayward' fruit as

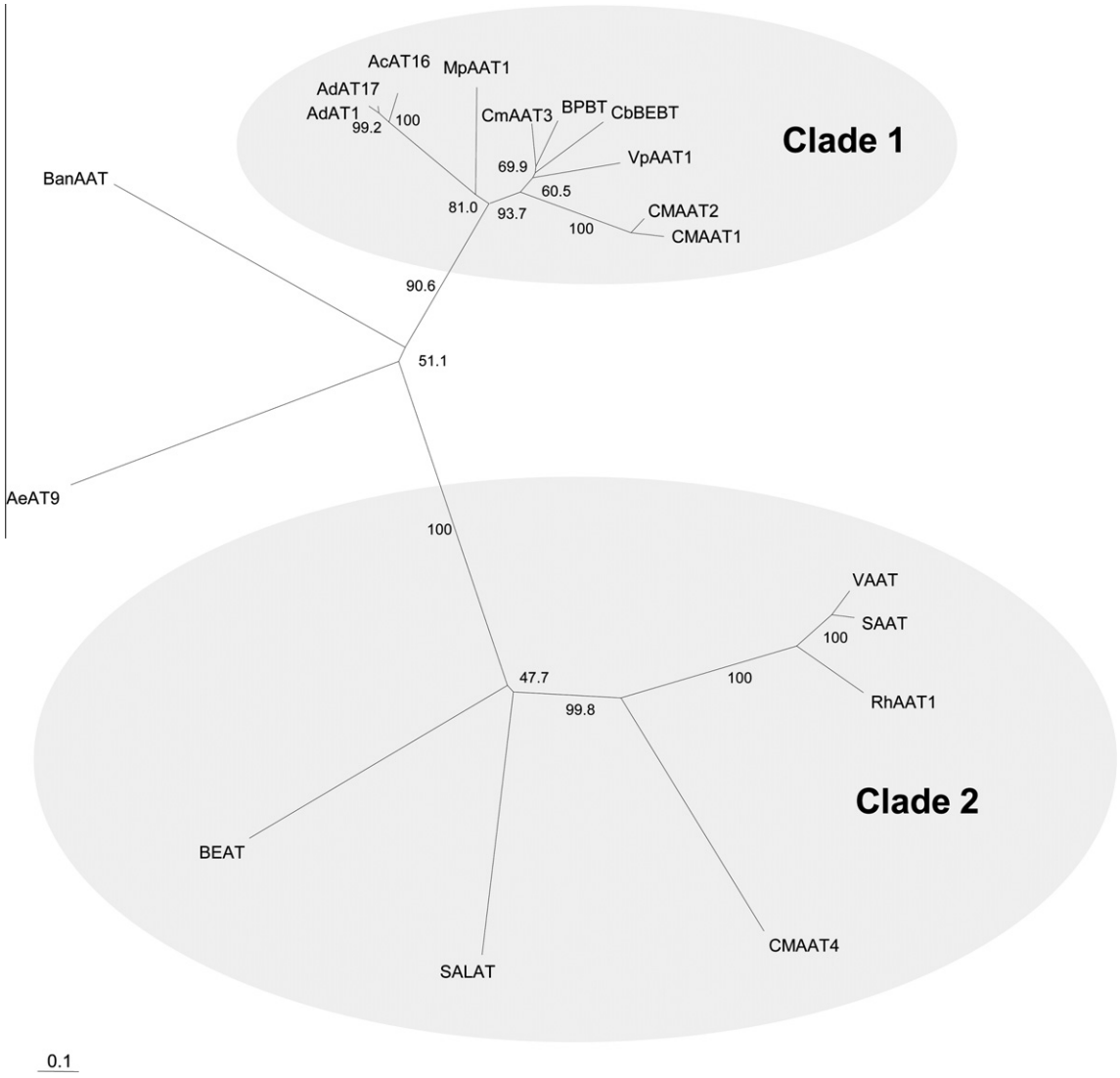

Fig. 6. Un-rooted phylogram of four *Actinidia* alcohol acyltransferases (AATs) with fruit- or flower-derived AATs from different plant species. The prefix indicates the species from which the sequence was originally isolated from (Ac: *A. chinensis*, Ad: *A. deliciosa*, Ae: *A. eriantha*). This tree is based on the amino acid alignment presented in Fig. 5 and percentage bootstrap values (1000 bootstrap replicates) for groupings are given for each branch.

described in Nieuwenhuizen et al. (2007). These fruits were harvested when mature but unripe. After harvest, fruits were either stored immediately at 20 °C to soften (non-ethylene untreated series) or treated with ethylene (100 μL L^{-1}) for 24 h and then stored at 20 °C to soften. For samples treated with ethylene, fruits were enclosed in an ethylene-free container for 1 h and the headspace gas analysed for ethylene production. Fruit producing >100 nL g FW^{-1} h^{-1} of ethylene were defined as climacteric (Nieuwenhuizen et al., 2007).

To determine the role of ethylene on putative *AT* and *AAT* expression in kiwifruit we used cDNA from an ACO silenced *A. chinensis* RNAi-line (T1) that was deficient in volatile ester production unless treated with exogenous ethylene as described in Atkinson et al. (2011). Briefly, fruits from transgenic and control lines were harvested when softening could be detected by hand (~24 weeks post anthesis). To synchronise fruit ripening, both control and transgenic fruit were treated with a short burst of exogenous ethylene (100 μL L^{-1}, 24 h), then held in an ethylene free environment at 20 °C. Exogenous climacteric ethylene production of individual fruit was monitored by placing fruit in 529-cm^3 respiration containers for 1 h. Headspace samples (1 ml) were taken using a syringe and measured by flame ionisation chromatography (PU 4500 Chromatograph, Phillips, UK) as described in Atkinson et al. (2011).

The cDNA was diluted 100-fold prior to use and negative controls without reverse transcriptase reaction were used to test for gDNA contamination. Transcription analysis of *Actinidia*-derived *AT* ESTs was performed relative to the reference gene Ubiquitin conjugating protein (UBC9) on a LightCycler® 480 platform using LightCycler® 480 SYBR Green master mix in a reaction volume of 5 μL. Four technical replicates were used and cDNA was replaced by water to test for false amplification. Any cycle threshold superior to 35 amplification cycles was considered as very low transcription and not considered for evaluation. A standard dilution series with plasmid DNA was generated to evaluate the primer efficiency of each primer which was greater than 1.9. The results were analysed using the LightCycler 480 software (Roche) and quantified according to Pfaffl (2001). Program: 1 min at 95 °C; 40 cycles of 10 s at 95 °C, 10 s at 60 °C, and 12 s at 72 °C; followed by melting curve analysis: 95 °C for 5 s, 65 °C for 60 s then ramping at 0.18 °C s^{-1} to 95 °C. Primers were designed within the open reading frame of the full-length contig. Primer sequences and predicted

product sizes are displayed in Table 2 (the prefix indicates the species from which the sequence was originally isolated; Aa: *A. arguta*, Ac: *A. chinensis*, Ad: *A. deliciosa,* Ae: *A. eriantha*, Ap: *A. polygama*).

4.3. Recombinant expression of Actinidia ATs in Saccharomyces cerevisiae

Following manufacturer's instructions (Invitrogen, pYES2.1 TOPO® TA Expression Kit), the selected sequences were cloned into the pYES2.1 TOPO® TA vector and verified by enzyme restriction analysis and sequencing. Protein sequence authenticity (AT1 (HO772635); AT16 (HO772640); AT9 (HO772637)) was confirmed for all clones although substitutions were noted for *AT9* (Ser^{407} to Ile) and *AT16* (Ala^{404} to Thr) which displayed a mutation in clear distance to the active site motif. A Kozac consensus sequence (TCCACAATGG) was linked to the start of each gene to facilitate translation in yeast (Miyasaka, 1999). Auto-ligated construct was used as negative control. The *S. cerevisiae* cell line INVSc1 (Invitrogen) was transformed with the pYES2.1 vector, harbouring the relevant construct. Vector containing the lacZ-gene was used as positive control for recombinant protein expression. Several precultures of the positive transformants were grown in selective SC-U minimal medium without uracil (Yeast Nitrogen Base, Difco) and 2% glucose at 30 °C and 250 rpm before gene induction. For recombinant expression, a culture with OD_{600} 0.4 was prepared in SC-U medium with 2% galactose and the conditions described above. Yeast cells were harvested by centrifugation (1800*g*, 10 min at 4 °C) after 20 h, flash frozen in liquid nitrogen and stored at −80 °C until needed.

4.4. Purification of recombinant Actinidia ATs

Cell pellets from a 400 mL cell culture were resuspended in 20 mL cold extraction buffer (20 mM $Na_2H_2PO_4$ at pH 7.2, 1 M NaCl, 10 mM imidazole, Complete™ protease inhibitor tablet-EDTA-free, Roche). The Emulsi- Flex-C5 high pressure homogeniser (AVESTIN Inc.) was used for cell disruption with a pressure setting between 15 and 20 kpsi. The homogenate was centrifuged at 10,000*g* for 30 min at 4 °C and the supernatant was filtered (0.2 μM Minisart®, Sartorium Stedim Biotech) before loading onto a 1 mL HiTrap FF column (GE Healthcare) using a peristaltic pump. Proteins were eluted from the Ni^{2+} resin with an imidazole gradient from 0 to 0.5 M using fast protein liquid chromatography (Äkta prime plus, GE Healthcare). The eluate-fractions were selected according to their OD_{280} in the range of 350–500 mM imidazole and Western Blot analysis was performed (Trans-Blot Semi-Dry Cell, Bio-Rad Laboratories), using anti-V5 (Invitrogen) as primary and anti-mouse IgG alkaline phosphatase conjugated IgG (H + L) (Promega) as the secondary antibody. Proteins were visualised using the 1-STEP™ NBT/BCIP alkaline phosphatase detection reagent (Pierce) according to the manufacturer's instructions. Proteins were quantified according to Bradford (1976). Initial optimisation of purification procedures included a desalting step but since this step resulted in significant protein losses and no difference in enzyme activity the step was dropped and not used for any of the results shown here.

Table 2
Primer sequences used for quantitative real-time RT-PCR analysis and their predicted product sizes.

Gene	Primer forward (5′-3′)	Primer Reverse (3′-5′)	Product size (bp)
UBC9	CCATTTCCAAGGTGTTGCTT	TACTTGTTCCGGTCCGTCTT	109
AaAT18	ACCCCGTCACAGTCATCAGAG	GCAATCCACCACAAGTTTTCG	107
AdAT2	CTCCCTCCATCACATTCCAG	CGGCATCTCCATAAACACG	199
AcAT15	ACCTCCCTCCATCACATTC	CGGCATCTCCATAAACACG	142
AdAT1	TCCCTTCATCCCATTCCAG	CGGCATCTCCATAAACACG	198
AdAT17	TGGCAGAGGGAGTTTCTAGC	TGGCTTCGAATGGCTCTTAT	160
AcAT16	AGGTTTTTCATACTTAGACG	TCACTCATTGTGTGGTTTAG	144
AcAT14	GCAGCAGAAATCCTCAAAG	GACGAAAGTCCTCAAAGTC	178
AdAT3	CCGACTCCAGAAATCAGAGC	CAGCTAGGCCGTCAACAAGT	153
AdAT7	CCGACTCCAGAAATCAGAG	CCCTAAACCAACACTAATGC	123
AcAT21	TGACACACCCAAACACAAC	TTAGGCCCGTAGAAGTAGAC	90
AdAT8	GACATCACACTCCCACCATTC	GGCTTTGAGAGAGTTGAGTTG	198
AcAT20	CTGAAAAGAGGTTGGAAAAC	ATGCCGTTGAAAAACTGAG	130
AeAT9	GAGTTAGCCACTGGCAGAGC	ACCCAGAAAGGTCAGGGACT	135
AcAT23	GGAGATGCCTTTGGTTGTTG	TGGCTTGCTTTGATGTTAGAG	150
AcAT24	TCAAGAGAAACCATCAAACC	CTGCGGCGTAGAAGTAGAC	122
AdAT6	ATGAAGGTTGAGGTGATTGC	ATGAGGAGTTGGAGAAGATG	57
AdAT11	GCCCACAGATTCCAGTAAACC	GTCAGAAGCACACAAGTAAGG	160
ApAT29	CCAGTCCAGTGAATGTGTTG	GAAGAATAGGCGTTGTGTG	140
AdAT22	GACGAGGGTGGTTGTGAAG	GGCAAACGGGTAAAAGTGAG	90
AcAT25	ATGAGGAGGGAGTGTTTAGGG	GCCAAAAGTGGTCTGTGAAG	184
AcAT28	CGACACCGTCTTCAATTCG	TTCCCAAGAATTTCGGAGTG	173
AeAT10	TGCCTTCTTCTTCTGTTTCC	GCCCTTTTGGATGTATTGG	128
AdAT12	GGGCGTCTTACTATCACAAC	GGCATCGTTACAGAGTATG	154
AcAT26	TGGCTTTCTCTCCTCTTGTG	GGCTTGGTGTTTATTTGGG	190
AcAT27	GTGGGGTCAGGTTCATTGAG	GTGGGGCACAAGCAACTTC	98
AcAT30	AAGTGTGGAGGATTATCAGTG	GGTGTTTGGCATTTTGAGAG	138

4.5. Enzyme assay and kinetic studies

To test for AAT-activity of the semi-purified extract, the combined fractions (350–500 mM imidazole) were assayed using HS-SPME and GC–MS. In a total volume of 1 mL 300 μL protein extract was mixed with assay buffer (20 mM $Na_2H_2PO_4$ at pH 8, 1 M NaCl, Complete™ protease inhibitor tablet-EDTA-free, Roche), alcohol mix (methanol, ethanol, propanol, butanol) containing 1 mM each, 5 μM of each internal standard ([D5]ethyl butyrate, ethyl 3-([D3]-methylsulfanyl)propionate) and acyl-CoA mix containing 100 μM of each CoA-substrate (acetyl-CoA, propionyl-CoA, butanoyl-CoA, hexanoyl-CoA, octanoyl-CoA, benzoyl-CoA, 2-(methylsulfanyl)acetyl-CoA and 3-(methylsulfanyl)propionyl-CoA) to start the reaction. These substrates were chosen because the corresponding esters were reported to occur in ripe kiwifruit. The samples were incubated at 30 °C for 1 h and kept on ice for 5 min before adding 100 μL of 10% SDS (w/v) solution which was confirmed to stop the enzyme reaction. The samples were immediately vortexed for 30 s, frozen in liquid nitrogen and stored at −20 °C until needed. Samples containing boiled protein and semi-purified, non-induced protein extract of each transformant were tested as negative controls. Different assay times (15 min–3 h) were tested to ensure optimum peak size and a linear increase in ester production rate (data not shown) and incubation for 1 h was found to be appropriate. In order to screen for preferred AAT-substrates of the recombinant protein, first an acyl-CoA mix was tested with each alcohol individually and second each individual acyl-CoA with a mixture of four alcohols. All samples were measured in duplicates.

The apparent catalytic efficiency (ACE) from semi-purified protein was defined as the initial slope of the enzyme reaction rate under limiting substrate conditions and mathematically responds to $V'_{max}\,K_m^{-1}$ (where V'_{max} is V_{max} of the semi-purified protein of unknown concentration). According to $k_{cat}\,K_m^{-1}$, $V'_{max}\,K_m^{-1}$ is a function of both the amount of enzyme present (V'_{max}) and the apparent K_m, and therefore regarded as an estimate of substrate specificity (Copeland, 2000). To separately calculate the enzyme kinetic parameters, acetyl-CoA substrate concentrations in the 3 mM range were necessary for AT16 using butanol. For our study it was not possible to use acyl-CoA substrates at these elevated concentrations because of the comparatively large reaction volume of the enzyme assay. Furthermore, these concentrations are not likely to be physiological and we therefore analysed the ACE in order to compare the substrate preferences of recombinant enzymes for

different substrates. The ACE was calculated either using a non-linear fit (Origin 7.5 SR4, Originlab Corporation) of the standard Michelis–Menten equation (Eq. (1)) when significant curvature in the v versus [S] response curve occurred or from the linear regression of the response of enzyme activity to substrate concentration as shown in Eqs. (1) and (2).

$$v = (V'_{max}/K_m) * [S]/([S]/K_m + 1) \quad (1)$$

At low substrate concentrations ($[S] \ll K_m$)

$$v = V'_{max}/K_m * [S] = ACE * [S] \quad (2)$$

where [S] is the substrate concentration in μM and V'_{max} is the enzyme activity in nkat (mg protein^{-1}).

4.6. Phylogenetic analysis

Eleven previously reported plant *AAT* genes from GenBank along with four *Actinidia AATs* (AT16 [HO772640], AT9 [HO772637], AT1 [HO772635], AT17 (HO772638)), isolated from *A. chinensis*, *A. deliciosa* and *A. eriantha* were analysed. Amino acid alignments of predicted proteins were constructed using Clustal X (Thompson et al., 1997). The presence of an active site histidine residue embedded in the HXXXD motif was checked in alignments. Phylogenetic analysis was carried out using the PHYLIP suite of programs and bootstrap analysis was conducted from 1000 bootstrap replicates using Seqboot (Felsenstein, 1993). Distances were calculated using Protdist, and the Fitch method was used to construct the unrooted tree. Treeview (v.1.6.6) was used to display results (Page, 1996). The GenBank protein accessions used in the alignment are included in Fig. 5.

Acknowledgements

The authors wish to thank Ross Atkinson and Niels Nieuwenhuizen for kindly providing cDNA aliquots. Furthermore, we acknowledge Ross Atkinson and Adam Matich for helpful comments to this manuscript and Jean-Claude Pech, William Laing and Laura Nicolau for their expert advice contributing to the success of this study. This work was funded by the New Zealand Foundation for Research Science and Technology (CO6X0403).

References

Aharoni, A., Keizer, L.C.P., Bouwmeester, H.J., Sun, Z., Alvarez-Huerta, M., Verhoeven, H.A., Blaas, J., van Houwelingen, A.M.M.L., De Vos, R.C.H., van der Voet, H., Jansen, R.C., Guis, M., Mol, J., Davis, R.W., Schena, M., van Tunen, A.J., O'Connell, A.P., 2000. Identification of the SAAT gene involved in strawberry flavor biogenesis by use of DNA microarrays. Plant Cell 12, 647–661.

Atkinson, R.G., Wang, M.Y., Luo, L., Wang, T., Norling, C.L., Johnston, S.L, Schröder, R., Schaffer, R.J., 2011. Dissecting the ripening process in an ethylene-knockdown kiwifruit (*Actinidia chinensis*) line. J. Exp. Bot., doi:10.1093/jxb/err063.

Balbontín, C., Gaete-Eastman, C., Fuentes, L., Figueroa, C.R., Herrera, R., Manriquez, D., Latché, A., Pech, J.-C., Moya-León, M.A., 2010. VpAAT1, a gene encoding an alcohol acyltransferase, is involved in ester biosynthesis during ripening of mountain papaya fruit. J. Agric. Food Chem. 58, 5114–5121.

Beekwilder, J., Alvarez-Huerta, M., Neef, E., Verstappen, F.W.A., Bouwmeester, H.J., Aharoni, A., 2004. Functional characterization of enzymes forming volatile esters from strawberry and banana. Plant Physiol. 135, 1865–1878.

Boatright, J., Negre, F., Chen, X.L., Kish, C.M., Wood, B., Peel, G., Orlova, I., Gang, D., Rhodes, D., Dudareva, N., 2004. Understanding *in vivo* benzenoid metabolism in *Petunia* petal tissue. Plant Physiol. 135, 1993–2011.

Bradford, M.M., 1976. A rapid and sensitive method for the quantitation of microgram quantities of protein utilizing the principle of protein–dye binding. Anal. Biochem. 72, 248–254.

Copeland, R.A., 2000. Enzymes, second ed. Wiley-VCH, New York.

Crowhurst, R.N., Gleave, A.P., MacRae, E.A., Ampomah-Dwamena, C., Atkinson, R.G., Beuning, L.L., Bulley, S.M., Chagne, D., Marsh, K.B., Matich, A.J., Montefiori, M., Newcomb, R.D., Schaffer, R.J., Usadel, B., Allan, A.C., Boldingh, H.L., Bowen, J.H., Davy, M.W., Eckloff, R., Ferguson, A.R., Fraser, L.G., Gera, E., Hellens, R.P., Janssen, B.J., Klages, K., Lo, K.R., MacDiarmid, R.M., Nain, B., McNeilage, M.A., Rassam, M., Richardson, A.C., Rikkerink, E.H., Ross, G.S., Schröder, R., Snowden, K.C., Souleyre, E.J.F., Templeton, M.D., Walton, E.F., Wang, D., Wang, M.Y., Wang, Y.Y., Wood, M., Wu, R., Yauk, Y.K., Laing, W.A., 2008. Analysis of expressed sequence tags from *Actinidia*: applications of a cross species EST database for gene discovery in the areas of flavor, health, color and ripening. BMC Genomics 9, 351.

D'Auria, J.C., 2006. Acyltransferases in plants: a good time to be BAHD. Curr. Opin. Plant Biol. 9, 331–340.

D'Auria, J.C., Chen, F., Pichersky, E., 2002. Characterization of an acyltransferase capable of synthesizing benzylbenzoate and other volatile esters in flowers and damaged leaves of *Clarkia breweri*. Plant Physiol. 130, 466–476.

Dudareva, N., D'Auria, J.C., Nam, K.H., Raguso, R.A., Pichersky, E., 1998. Acetyl-CoA:benzylalcohol acetyltransferase – an enzyme involved in floral scent production in *Clarkia breweri*. Plant J. 14, 297–304.

El-Sharkawy, I., Manriquez, D., Flores, F.B., Regad, F., Bouzayen, M., Latche, A., Pech, J.C., 2005. Functional characterization of a melon alcohol acyl-transferase gene family involved in the biosynthesis of ester volatiles. Identification of the crucial role of a threonine residue for enzyme activity. Plant Mol. Biol. 59, 345–362.

Felsenstein, J., 1993. PHYLIP (Phylogeny Inference Package), Version 3.6a2. (Department of Genetics). University of Washington, Seattle. Distributed by the author at <http://evolution.genetics.washington.edu/phylip.html>.

Friel, E.N., Wang, M., Taylor, A.J., MacRae, E.A., 2007. *In vitro* and *in vivo* release of aroma compounds from yellow-fleshed kiwifruit. J. Agric. Food. Chem. 55, 6664–6673.

Gilbert, J.M., Young, H., Ball, R.D., Murray, S.H., 1996. Volatile flavour compounds affecting consumer acceptability of kiwifruit. J. Sens. Stud. 11, 247–259.

Grothe, T., Lenz, R., Kutchan, T.M., 2001. Molecular characterization of the salutaridinol 7-*O*-acetyltransferase involved in morphine biosynthesis in opium poppy *Papaver somniferum*. J. Biol. Chem. 276, 30717–30723.

Günther, C.S., Matich, A.J., Marsh, K.B., Nicolau, L., 2010. (Methylsulfanyl) alkanoate ester biosynthesis in *Actinidia chinensis* kiwifruit and changes during cold storage. Phytochemistry 71, 742–750.

Günther, C.S., Heinemann, K., Laing, W., Nicolau, L., Marsh, K.B., 2011. Ethylene-regulated (methylsulfanyl)alkanoate ester biosynthesis is likely to be modulated by precursor availability in Actinidia chinensis genotypes. J. Plant Physiol. 168, 629–638.

Hartmann, T., 2007. From waste products to ecochemicals: fifty years research of plant secondary metabolism. Phytochemistry 68, 2831–2846.

Ma, X.Y., Koepke, J., Panjikar, S., Fritzsch, G., Stockigt, J., 2005. Crystal structure of vinorine synthase, the first representative of the BAHD superfamily. J. Biol. Chem. 280, 13576–13583.

Miyasaka, H., 1999. The positive relationship between codon usage bias and translation initiation AUG context in *Saccharomyces cerevisiae*. Yeast 15, 633–637.

Morton, I.D., Macleod, A.J., 1990. Food Flavours, the Flavour of Fruits. Elsevier, Amsterdam–Oxford–New York–Tokyo.

Nieuwenhuizen, N.J., Beuning, L.L., Sutherland, P.W., Sharma, N.N., Cooney, J.M., Bieleski, L.R.F., Schrodera, R., MacRae, E.A., Atkinson, R.G., 2007. Identification and characterisation of acidic and novel basic forms of actinidin, the highly abundant cysteine protease from kiwifruit. Funct. Plant Biol. 34, 946–961.

Page, R.D.M., 1996. Treeview: an application to display phylogenetic trees on personal computers. Comput. Appl. Biosci. 12, 357–358.

Peach, K., 1950. Biochemie und Physiology der sekundären Pflanzenstoffe. Springer, Berlin Gottingen, Heidelberg.

Pfaffl, M.W., 2001. A new mathematical model for relative quantification in real-time RT-PCR. Nucleic Acids Res. 29.

Shalit, M., Guterman, I., Volpin, H., Bar, E., Tamari, T., Menda, N., Adam, Z., Zamir, D., Vainstein, A., Weiss, D., Pichersky, E., Lewinsohn, E., 2003. Volatile ester formation in roses. Identification of an acetyl-coenzyme A. Geraniol/citronellol acetyltransferase in developing rose petals. Plant Physiol. 131, 1868–1876.

Souleyre, E.J.F., Günther, C.S., Wang, M.Y., Newcomb, R., Marsh, K.B., 2011. Ester biosynthesis in kiwifruit-from genes to enzymes to pathways. Acta Horticulturae, 7th International Symposium on Kiwifruit.

Souleyre, E.J.F., Greenwood, D.R., Friel, E.N., Karunairetnam, S., Newcomb, R.D., 2005. An alcohol acyl transferase from apple (cv. Royal Gala), MpAAT1, produces esters involved in apple fruit flavor. FEBS J. 272, 3132–3144.

St-Pierre, B., De Luca, V., 2000. Evolution of acyltransferase genes: origin and diversification of the BAHD superfamily of acyltransferases involved in secondary metabolism. In: Ibrahim, R., Varin, L., De Luca, V., Romeo, J.T. (Eds.), Recent Advances in Phytochemistry Evolution of Metabolic Pathways, vol. 34, pp. 285–315.

Thompson, J.D., Gibson, T.J., Plewniak, F., Jeanmougin, F., Higgins, D.G., 1997. The CLUSTAL_X windows interface: flexible strategies for multiple sequence alignment aided by quality analysis tools. Nucleic Acids Res. 25, 4876–4882.

Wang, M.Y., MacRae, E., Wohlers, M., Marsh, K.B., 2011. Changes in volatile production and sensory quality of kiwifruit during fruit maturation in *Actinidia deliciosa* 'Hayward' and *A. chinensis* 'Hort16A'. Postharv. Biol. Technol. 59, 16–24.

Whittaker, D.J., Smith, G.S., Gardner, R.C., 1997. Expression of ethylene biosynthetic genes in *Actinidia chinensis* fruit. Plant Mol. Biol. 34, 45–55.

Young, H., Paterson, V.J., 1985. The effects of harvest maturity, ripeness and storage on kiwifruit aroma. J. Sci. Food Agric. 36, 352–358.